Inorganic Chemistry

Article

pubs.acs.org/IC

Oscillator Strength of Symmetry-Forbidden d-d Absorption of Octahedral Transition Metal Complex: Theoretical Evaluation

Ken Saito,[†] Yoshinori Eishiro,[†] Yoshihide Nakao,[†] Hirofumi Sato,[†] and Shigeyoshi Sakaki*[,‡]

[†]Department of Molecular Engineering, Graduate School of Engineering, Kyoto University, Nishikyo-ku, Kyoto 615-8510, Japan

[‡]Fukui Institute for Fundamental Chemistry, Kyoto University, Nishihiraki-cho, Takano, Sakyo-ku, Kyoto 606-8103, Japan

Supporting Information

ABSTRACT: The theoretical evaluation of the oscillator strength of a symmetry-forbidden d-d transition is not easy even nowadays. A new approximate method is proposed here and applied to octahedral complexes $[Co(NH_3)_6]^{3+}$ and $[Rh(NH_3)_6]^{3+}$ as an example. Our method incorporates the effects of geometry distortion induced by molecular vibration and the thermal distribution of such distorted geometries but does not need the Herzberg−Teller approximation. The calculated oscillator strengths of $[Co(NH_3)_6]^{3+}$ agree well with the experimental values in both $^1A_{1g} \rightarrow {}^1T_{1g}$ and $^1A_{1g} \rightarrow {}^1T_{2g}$ transitions. In the Rh analogue, though the calculated oscillator strengths are somewhat smaller than the experimental values, computational results reproduce well the experimental trends that the oscillator strengths of $[Rh(NH_3)_6]^{3+}$ are much larger than those of the Co analogue and the oscillator strength of the $^1A_{1g} \rightarrow {}^1T_{1g}$ transition is larger than that of the $^1A_{1g} \rightarrow {}^1T_{2g}$ transition. It is clearly shown that the oscillator strength is not negligibly small even at 0 K because the distorted geometry (or the uncertainty in geometry) by zero-point vibration contributes to the oscillator strength at 0 K. These results are discussed in terms of frequency of molecular vibration, extent of distortion induced by molecular vibration, and charge-transfer character involved in the d-d transition. The computational results clearly show that our method is useful in evaluating and discussing the oscillator strength of symmetry-forbidden d-d absorption of transition metal complex.

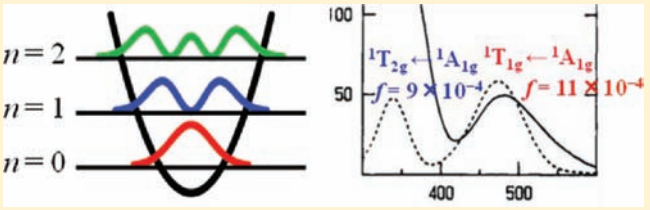

INTRODUCTION

Absorption spectra of transition metal complexes can be easily investigated nowadays with electronic structure theory such as time-dependent density functional theory (TD-DFT)[1] and symmetry-adapted cluster expansion followed by configuration interaction (SAC/SAC−CI) method[2]. However, the oscillator strength of a symmetry-forbidden transition such as a d-d transition of a transition metal complex bearing inversion symmetry cannot be evaluated with the usual electronic structure theory, as is well-known.[3,4] In a real molecule, however, geometry is not frozen but thermally vibrating. Some of the molecular vibrations break the symmetry of geometry in which the transition dipole moment of the d-d transition becomes nonzero even in a metal complex with the inversion symmetry. In other words, the d-d absorption is induced by molecular vibration. This means that the oscillator strength of the symmetry-forbidden d-d transition can be theoretically evaluated by incorporating effects of molecular vibration into the electronic structure calculation. However, such theoretical evaluations have been limited, so far. One of the pioneering theoretical works was reported by Kato, Iuchi, and their collaborators.[5] They investigated the d-d absorption spectrum of octahedral $[Ni(H_2O)_6]^{2+}$ with a model Hamiltonian which was constructed by molecular dynamics simulation. Another example[6] was a theoretical study of the d-d absorption spectrum of square planar $[PtCl_4]^{2-}$ with the Hertzberg−Teller (HT) approximation.[7] In this study, the Taylor expansion of transition dipole M by normal coordinate Q_i is truncated at the second term and then the M value is calculated with the derivative of M by Q_i, $(\partial M/\partial Q_i)$, and the vibrational wave functions in the electronic ground and excited states; see ref 8 for more details. Considering that the oscillator strength of symmetry-forbidden d-d transition has not been evaluated except for these studies, its theoretical evaluation is challenging even nowadays. Remember that the d-d absorption spectrum provides us with important knowledge of the d-d orbital energy gap. To present a correct assignment of the d-d absorption, the oscillator strength is indispensable. Thus, it is important to investigate theoretically the d-d absorption and its oscillator strength.

In this study, we wish to propose a new method to evaluate the oscillator strength of the symmetry-forbidden d-d transition. In our method, the geometry distribution around the equilibrium geometry is incorporated by considering the vibrational wave function, while the HT approximation was not employed. The Boltzmann distribution law was employed to evaluate the population of vibrationally excited state. This method was applied to octahedral transition metal complexes, $[Co(NH_3)_6]^{3+}$ and $[Rh(NH_3)_6]^{3+}$, as an example. Though these compounds are not of that much interest, we calculated the oscillator strength of these well-known compounds here

Received: August 10, 2011
Published: February 22, 2012

   dx.doi.org/10.1021/ic2017402 | Inorg. Chem. 2012, 51, 2785−2792

Scheme 1

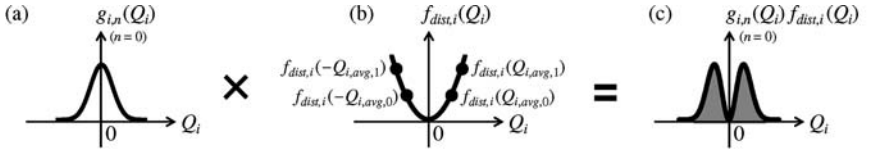

Probability of distorted geometry by zero-point vibration

Oscillator strength as a function of coordinate Q_i

Dark area indicates corresponds $f_{i,n=0}$ in eq 2.

because this is the first application of our method. Our purposes here are to examine whether or not our method is useful in evaluating the oscillator strengths of symmetry-forbidden d-d transitions, $^1A_{1g} \rightarrow {}^1T_{1g}$ and $^1A_{1g} \rightarrow {}^1T_{2g}$, of an octahedral transition metal complex,[9] to elucidate what kinds of molecular vibrations contribute to their oscillator strengths, to evaluate contribution of zero-point vibration, and to show how much temperature influences the oscillator strength.

METHOD AND COMPUTATIONAL DETAILS

DFT Calculations. The core electrons of Co (up to 2p) and Rh (up to 3d) were replaced with the Stuttgart–Dresden–Bonn relativistic effective core potentials (SDB ECPs),[10,11] and their valence electrons were represented with (311111/22111/4111/11) basis sets.[10−12] The cc-pVDZ basis sets[13] were used for H and N.

Geometries of $[Co(NH_3)_6]^{3+}$ and $[Rh(NH_3)_6]^{3+}$ in the $^1A_{1g}$ ground state were optimized with the DFT method, where the B3PW91 functional[14,15] was employed. Their vibration frequencies were evaluated with the same method. Excitation energies of the $^1A_{1g} \rightarrow {}^1T_{1g}$ and $^1A_{1g} \rightarrow {}^1T_{2g}$ absorptions were evaluated with the TD-DFT(B3PW91) method.[16,17]

All electronic structure calculations were performed by the Gaussian 03 and 09 program packages,[18] where the numerical integrals were calculated with the "UltraFine grid" (99 × 590) and the geometry optimizations were carried out in the "VeryTight" convergence criteria in the Gaussian programs. The evaluated frequencies and force constants were corrected with scaling factors, 0.9573 and 0.9164, respectively.[19] Molecular orbitals were drawn by the MOLEKEL program.[20]

Procedure to Evaluate Oscillator Strength of Symmetry-Forbidden d–d Transition. To calculate the oscillator strength explicitly, we need vibrational wave functions at the ground and excited states. However, it is not easy to calculate the potential energy surface and vibrational wave function in the excited states of $[Co(NH_3)_6]^{3+}$ and the Rh analogue because their excited states induce the Jahn–Teller distortion. Here, we wish to propose an approximate way to evaluate the oscillator strength of the symmetry-forbidden d-d transition. In our method, the oscillator strength is calculated with distorted geometry along the normal coordinate of fundamental vibration, as will be discussed below. This is the same as the usual calculation of symmetry-allowed transition in which the Franck–Condon factor is not considered explicity but assumed to be 1.0. However, the potential energy surface and the vibrational wave function of the excited state were not considered in our method.[21] Because of these approximations, our method is not perfect and its application is limited; for instance, it can not be applied to the evaluation of shape and vibrational structure of absorption spectrum which arises from vibronic coupling. Also, the present method is not useful to make a comparison of absorption spectrum between two complexes when the potential energy surface in the excited state is considerably different between them. In addition, note that, in our method, the Jahn–Teller effect of the excited state is ignored,[21] which influences the absorption spectrum.[22] Despite of these defects, we believe that the present procedure has some practical merit.

As well-known, the probability $g_{i,n}(Q_i)$ of distorted geometry is determined by the square of the vibrational wave function $\chi_{i,n}(Q_i)$;[21]

$$g_{i,n}(Q_i) = |\chi_{i,n}(Q_i)|^2 \tag{1}$$

where n (= 0, 1, 2,...) is quantum number of the vibrational wave function and Q_i is normal mode coordinate associated with the fundamental vibration mode i. Equilibrium geometry corresponds to $Q_i = 0$. The probability of distorted geometry in zero-point vibration is schematically shown in Scheme 1a, as an example.

The inversion center of the octahedral complex disappears with some of molecular vibrations. In such distorted geometry, the oscillator strengths of the $^1A_{1g} \rightarrow {}^1T_{1g}$ and $^1A_{1g} \rightarrow {}^1T_{2g}$ transitions become nonzero.[9] The oscillator strength $f_{dist,i}(Q_i)$ at distorted geometry Q_i was calculated with the TD-DFT method,[23] where the distorted geometrical coordinate Q_i was determined along the normal mode i at an appropriate interval; note that the normal mode i is provided by the Gaussian program package, where the harmonic oscillator approximation is employed. All vibration modes were considered unless otherwise the contribution to the distorted geometry is negligibly small; See Supporting Information page S4 for details of evaluation of $f_{dist,i}(Q_i)$.

The oscillator strength $f_{i,n}$ induced by vibration mode i with quantum number n is represented by the integral of the product of $f_{dist,i}(Q_i)$ and $g_{i,n}(Q_i)$, as shown by eq 2;

$$f_{i,n} = \int_{-\infty}^{\infty} g_{i,n}(Q_i) f_{dist,i}(Q_i)\, dQ_i \tag{2}$$

For instance, the $f_{i,0}$ value corresponds to a dark area in Scheme 1c. This integral was calculated numerically; see also Supporting Information page S4.

The population $P_{i,n}$ of the n-th vibrationally excited state in the vibration mode i depends on temperature T, according to the Boltzmann distribution law. Because the harmonic oscillator approximation is employed here, the population $P_{i,n}$ is described by eq 3

$$P_{i,n}(T) = \frac{\exp[-(n + 1/2)\hbar\omega_i/(k_B T)]}{\sum_j \exp[-(j + 1/2)\hbar\omega_i/(k_B T)]} \tag{3}$$

where k_B is the Boltzmann constant, $\hbar$ is the reduced Planck constant, and ω_i is the frequency of vibration of mode i. The oscillator strength $f_i(T)$ induced by vibration mode i at temperature T is represented by the sum of the product of $f_{i,n}$ and $P_{i,n}(T)$;

$$f_i(T) = \sum_{n=0}^{\infty} P_{i,n}(T) f_{i,n} \tag{4}$$

The sum of the $f_i(T)$ values on all fundamental vibrations corresponds to the total oscillator strength $f(T)$ at temperature T

$$f(T) = \sum_i f_i(T) \tag{5}$$

Here, the mode coupling is not considered after checking that it is not large; see Supporting Information page S4. Two-photon excitation is not considered also, indicating that some of intensity is missed.

dx.doi.org/10.1021/ic2017402 | Inorg. Chem. 2012, 51, 2785–2792

RESULTS AND DISCUSSION

Optimized Geometries and d-d Absorption Spectra of $[Co(NH_3)_6]^{3+}$ and $[Rh(NH_3)_6]^{3+}$. Optimized M−N bond lengths of $[Co(NH_3)_6]^{3+}$ and $[Rh(NH_3)_6]^{3+}$ are 2.009 and 2.113 Å, respectively, as shown in Table 1, which agree well with the experimental values (1.967 and 2.071 Å).[24,25] The excitation energies of $[Co(NH_3)_6]^{3+}$ are evaluated to be 2.61 and 3.62 eV for the $^1A_{1g} \rightarrow {}^1T_{1g}$ and $^1A_{1g} \rightarrow {}^1T_{2g}$ transitions, respectively, which also agree well with the experimental values (2.62 and 3.67 eV).[26] Those of $[Rh(NH_3)_6]^{3+}$ are evaluated to be 3.92 and 4.54 eV for the $^1A_{1g} \rightarrow {}^1T_{1g}$ and $^1A_{1g} \rightarrow {}^1T_{2g}$ transitions, respectively. The former energy is almost the same as the experimental value (4.03 eV).[27] Though the latter one is moderately lower than the experimental value (4.86 eV),[27] the difference is not large (about 0.3 eV).

Table 1. Optimized Bond Lengths (in Å) and Absorption Energies (in eV) of $[Co(NH_3)_6]^{3+}$ and $[Rh(NH_3)_6]^{3+}$

		calcd.	expt.
$[Co(NH_3)_6]^{3+}$	r(Co−N)	2.009	1.967[a]
	$\Delta E(^1A_{1g} \rightarrow {}^1T_{1g})$	2.61	2.62[b]
	$\Delta E(^1A_{1g} \rightarrow {}^1T_{2g})$	3.62	3.67[b]
$[Rh(NH_3)_6]^{3+}$	r(Rh−N)	2.113	2.071[c]
	$\Delta E(^1A_{1g} \rightarrow {}^1T_{1g})$	3.92	4.03[d]
	$\Delta E(^1A_{1g} \rightarrow {}^1T_{2g})$	4.54	4.86[d]

[a]Ref 24. [b]Ref 26. These absorption energies were measured in 5.0 M ammonia−water at 293 K. [c]Ref 25. [d]Ref 27. These absorption energies were measured in aqueous solution at room temperature.

The oscillator strengths of $[Co(NH_3)_6]^{3+}$ at 293 K are evaluated to be 11.1×10^{-4} and 8.1×10^{-4} for the $^1A_{1g} \rightarrow {}^1T_{1g}$ and $^1A_{1g} \rightarrow {}^1T_{2g}$ transitions, respectively, as shown in Table 2. These results agree well with the experimental values (11×10^{-4} and 9×10^{-4}).[26]

In $[Rh(NH_3)_6]^{3+}$, the oscillator strengths are evaluated to be 22.7×10^{-4} and 13.0×10^{-4} for the $^1A_{1g} \rightarrow {}^1T_{1g}$ and $^1A_{1g} \rightarrow {}^1T_{2g}$ transitions, respectively. Though these values are somewhat smaller than the experimental values (36×10^{-4} and 27×10^{-4}),[27,28] the experimental trend of the oscillator strength is reproduced well, as follows: In both of experimental and theoretical results, the oscillator strengths of the $^1A_{1g} \rightarrow {}^1T_{1g}$ transitions of $[Co(NH_3)_6]^{3+}$ and $[Rh(NH_3)_6]^{3+}$ are somewhat larger than those of the $^1A_{1g} \rightarrow {}^1T_{2g}$ transitions and the oscillator strengths of $[Rh(NH_3)_6]^{3+}$ are considerably larger than those of $[Co(NH_3)_6]^{3+}$ in both of the $^1A_{1g} \rightarrow {}^1T_{1g}$ and $^1A_{1g} \rightarrow {}^1T_{2g}$ transitions. These results indicate that our method is useful in evaluating and discussing the oscillator strength of the symmetry-forbidden d-d absorption, at least semiquantitatively.

Oscillator Strength at 0 K and Contributions of Various Molecular Vibration Modes. It is of considerable interest to investigate whether or not the symmetry-forbidden d-d absorption can be observed at 0 K because vibration does not occur at 0 K in a classical sense. However, the oscillator strength of $[Co(NH_3)_6]^{3+}$ is evaluated to be 4.6×10^{-4} and 4.1×10^{-4} for the $^1A_{1g} \rightarrow {}^1T_{1g}$ and $^1A_{1g} \rightarrow {}^1T_{2g}$ transitions, respectively, at 0 K, as shown in Table 2, though they are considerably smaller than those at 293 K (11.1×10^{-4} and 8.1×10^{-4}), as expected. The oscillator strength of $[Rh(NH_3)_6]^{3+}$ at 0 K is evaluated to be 11.7×10^{-4} and 7.6×10^{-4} for the $^1T_{1g}$ and $^1T_{2g}$ transitions, respectively, which are also considerably smaller than the values at 293 K (22.7×10^{-4} and 13.0×10^{-4}). It is noted that though these oscillator strengths at 0 K are considerably smaller than at 298 K they are not negligibly small but instead are 40 to 60% of the oscillator strengths at 298 K. This means that the symmetry-forbidden d-d absorption can be observed even at 0 K. This is because the zero-point vibration provides the distribution of distorted geometry around the equilibrium geometry even at 0 K, which corresponds to the uncertainty of geometry around the equilibrium geometry at 0 K. Such distribution of distorted geometry contributes to the oscillator strength of the symmetry-forbidden d-d transition. In other words, the zero-point vibration plays an important role in the symmetry-forbidden d-d transition.

It is of considerable interest to clarify what vibration mode contributes to the oscillator strength at 0 K. In the octahedral molecule, there are such six fundamental vibration modes as the symmetric stretching mode (A_{1g}), symmetric degenerate stretching mode (E_g), symmetric degenerate bending mode (T_{2g}), antisymmetric degenerate stretching mode (T_{1u}), and two kinds of antisymmetric degenerate bending modes (T_{1u} and T_{2u}),[29] as shown in Schemes 2a and 2b. Because the symmetry of the former three vibrational modes is gerade, the

Table 2. Oscillator Strengths (in $\times 10^{-4}$) of the $^1A_{1g} \rightarrow {}^1T_{1g}$ and $^1A_{1g} \rightarrow {}^1T_{2g}$ absorptions of $[Co(NH_3)_6]^{3+}$ and $[Rh(NH_3)_6]^{3+}$

	$[Co(NH_3)_6]^{3+}$				$[Rh(NH_3)_6]^{3+}$			
	0 K		293 K		0 K		293 K	
	$^1T_{1g}$	$^1T_{2g}$	$^1T_{1g}$	$^1T_{2g}$	$^1T_{1g}$	$^1T_{2g}$	$^1T_{1g}$	$^1T_{2g}$
experimental oscillator strength			11[a]	9[a]			36[b]	27[b]
calculated oscillator strength	4.6	4.1	11.1	8.1	11.7	7.6	22.7	13.0
details of the calculated oscillator strength								
M−NH_3 asym deg stretching (T_{1u}) (3)[c,d]	0.0	0.5	0.0	0.8	0.2	0.7	0.3	1.0
H_3N−M−NH_3 asym deg bending (T_{1u}) (3)[c,d]	1.2	0.8	1.9	1.4	3.0	2.0	5.4	3.6
H_3N−M−NH_3 asym deg bending (T_{2u}) (3)[c,d]	0.8	0.6	1.7	1.3	2.3	1.2	5.2	2.6
rotational vibration around M−NH_3 axis (3)[d]	0.5	0.3	5.2	2.8	0.6	0.3	6.0	2.3
M−NH_3 wagging (6)[d]	1.7	1.4	1.8	1.5	4.1	2.5	4.3	2.6
N−H stretching in NH_3 ligands (9)[d]	0.3	0.3	0.3	0.3	1.2	0.7	1.2	0.7
H−N−H bending in NH_3 ligands (9)[d]	0.2	0.2	0.2	0.2	0.4	0.3	0.4	0.3

[a]Ref 26. These absorption spectra were measured in 5.0 M ammonia−water at 293 K. [b]Ref 27. These absorption spectra were measured in aqueous solution at room temperature. [c]The term "asym deg" means "antisymmetric degenerate". [d]Numbers in parentheses represent numbers of fundamental vibration modes bearing the ungerade symmetry. Calculated oscillator strengths are the sum of the oscillator strengths provided by each fundamental vibration. See footnote 29 for details.

dx.doi.org/10.1021/ic2017402 | Inorg. Chem. 2012, 51, 2785−2792

Scheme 2

(a) Characteristic vibration modes of octahedral molecule with gerade symmetry

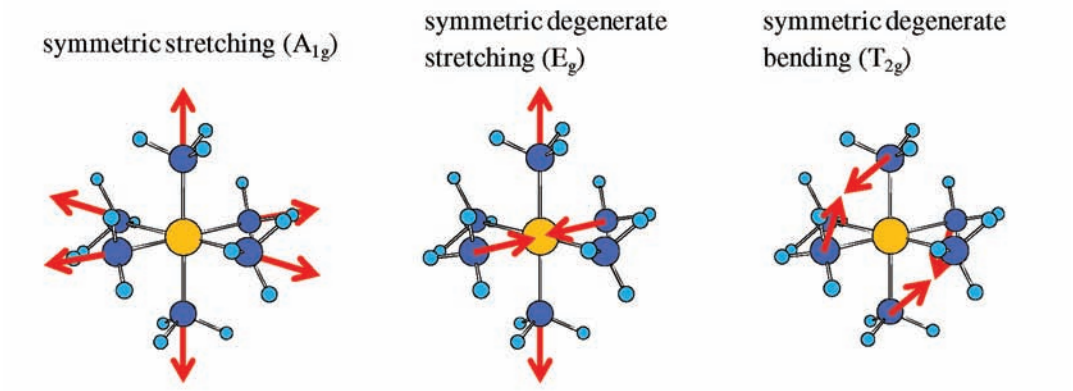

(b) Characteristic vibration modes of octahedral molecule with ungerade symmetry

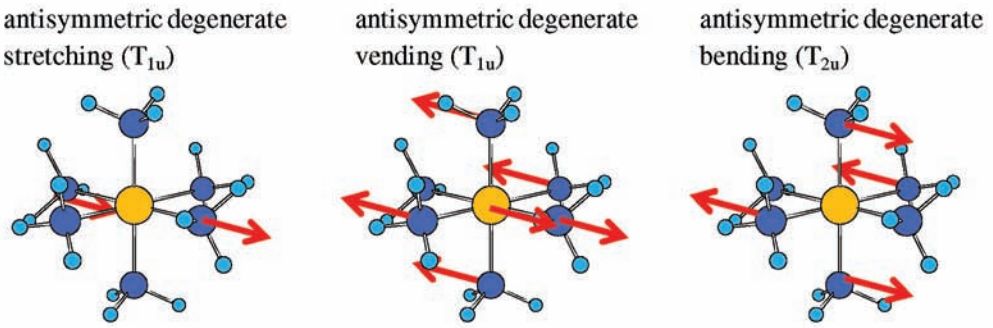

(c) Other vibration modes

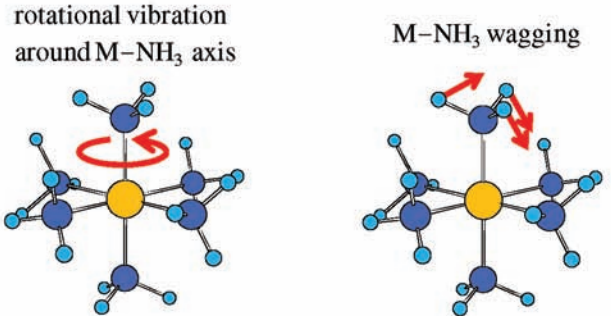

Though only one M−NH_3 ligand vibrates in left schemes for brevity, six M−NH_3 ligands vibrate in real molecule.

oscillator strength is not provided at all by these vibration modes. On the other hand, the latter three vibrational modes, whose symmetry is ungerade, contribute to the oscillator strengths of the symmetry-forbidden d-d transition. In $[Co(NH_3)_6]^{3+}$, two kinds of degenerate antisymmetric H_3N−Co−NH_3 bending vibrations of T_{1u} and T_{2u} considerably contribute to the oscillator strength of the d-d absorption at 0 K, as shown in Table 2, because the considerably large geometrical distortion is induced by these vibrations; the oscillator strength induced by the T_{1u} bending mode is 1.2×10^{-4} and 0.8×10^{-4} for the $^1A_{1g} \rightarrow {}^1T_{1g}$ and $^1A_{1g} \rightarrow {}^1T_{2g}$ transitions, respectively, and that induced by the T_{2u} bending mode is 0.8×10^{-4} and 0.6×10^{-4} for the $^1A_{1g} \rightarrow {}^1T_{1g}$ and $^1A_{1g} \rightarrow {}^1T_{2g}$ transitions.[29] On the other hand, the degenerate antisymmetric Co−NH_3 stretching vibration mode of T_{1u} contributes much less to the oscillator strength because the distortion is not large; for instance, the oscillator strength induced by this vibration mode is 0.0 and 0.5×10^{-4} for the $^1A_{1g} \rightarrow {}^1T_{1g}$ and $^1A_{1g} \rightarrow {}^1T_{2g}$ transitions, respectively.

There are several other vibration modes which induce little distortion from the octahedral geometry. One of such vibration modes is the M−NH_3 wagging mode; see Scheme 2c. Interestingly, this vibration mode contributes considerably to the oscillator strength of the d-d absorption, as follows; the oscillator strength induced by this vibration mode is 1.7×10^{-4} and 1.4×10^{-4} for the $^1A_{1g} \rightarrow {}^1T_{1g}$ and $^1A_{1g} \rightarrow {}^1T_{2g}$ transitions, respectively, in $[Co(NH_3)_6]^{3+}$ at 0 K, as shown in Table 2. Also, the M−NH_3 rotational vibration around the M−NH_3 bond axis (Scheme 2c)[30] contributes somewhat to the oscillator strength at 0 K, though this vibration distorts the octahedral geometry much less than the M-NH_3 wagging mode; the oscillator strength induced by this vibration mode is evaluated to be 0.5×10^{-4} and 0.3×10^{-4} for the $^1A_{1g} \rightarrow {}^1T_{1g}$ and $^1A_{1g} \rightarrow {}^1T_{2g}$ transitions, respectively, as shown in Table 2.

dx.doi.org/10.1021/ic2017402 | Inorg. Chem. 2012, 51, 2785−2792

Table 3. Wavenumbers (in cm^{-1}) and Populations of the Ground and Excited Vibrational States at 293 K

	$[Co(NH_3)_6]^{3+}$			$[Rh(NH_3)_6]^{3+}$		
		population			population	
	wavenumber[a]	ground state	excited state[b]	wavenumber[a]	ground state	excited state[b]
M−NH_3 asym deg stretching (T_{1u}) (3)[c,d]	400−402	0.86	0.14	395−397	0.86	0.14
H_3N−M−NH_3 asym deg bending (T_{1u}) (3)[c,d]	288−289	0.76	0.24	254−255	0.71	0.29
H_3N−M−NH_3 asym deg bending (T_{2u}) (3)[c,d]	199−209	0.62−0.64	0.36−0.38	189−196	0.61−0.62	0.38−0.39
rotational vibration around M−NH_3 axis (3)[c]	42−128	0.19−0.47	0.53−0.81	47−107	0.21−0.41	0.59−0.79
M−NH_3 wagging (6)[d]	702−765	0.97−0.98	0.03−0.02	732−774	0.97−0.98	0.02−0.03
N−H stretching in NH_3 ligands (9)[d]	3260−3345	1.00	0.00	3260−3344	1.00	0.00
H−N−H bending in NH_3 ligands (9)[d]	1340−1606	1.00	0.00	1344−1602	1.00	0.00

[a]See refs 30 and 31 for details. [b]This population corresponds to the sum of the populations of the all vibrational excited states (n = 1, 2, 3,...). [c]The term "asym deg" means "antisymmetric degenerate". [d]Numbers in parentheses represent the numbers of fundamental vibration modes bearing the ungerade symmetry..

Not only the M−NH_3 bonds but also the N−H bonds of the NH_3 ligands contribute to oscillator strength. Such vibrations are N−H stretching and H−N−H bending modes. As shown in Table 2, the oscillator strengths induced by the N−H stretching and H−N−H bending modes are evaluated to be 0.3×10^{-4} and 0.2×10^{-4} for the $^1A_{1g} \rightarrow {}^1T_{1g}$ and $^1A_{1g} \rightarrow {}^1T_{2g}$ transitions, respectively, at 0 K. In other words, both vibration modes contribute somewhat to the oscillator strength of the d-d transitions of $[Co(NH_3)_6]^{3+}$.

In $[Rh(NH_3)_6]^{3+}$, the molecular vibrations contribute similarly to the oscillator strength at 0 K like in the Co analogue, as follows: Two kinds of degenerate antisymmetric H_3N−Rh−NH_3 bending modes (T_{1u} and T_{2u}) contribute considerably to the oscillator strengths of the $^1A_{1g} \rightarrow {}^1T_{1g}$ and $^1A_{1g} \rightarrow {}^1T_{2g}$ transitions, as shown in Table 2.[31] On the other hand, the degenerate antisymmetric Rh−NH_3 stretching mode of T_{1u} contributes little to the oscillator strength. The Rh−NH_3 wagging vibration contributes considerably to the oscillator strength, though this vibration distorts little the octahedral geometry. The Rh−NH_3 rotational vibration around the Rh−NH_3 axis and the vibrations in the NH_3 ligand moieties contribute somewhat to the oscillator strength of the d-d transition at 0 K.

Temperature Dependence of Oscillator Strength. Here, we wish to discuss what vibration mode contributes to the increase in oscillator strength by temperature. The rotational vibrations around the M−NH_3 bond axis significantly increase the oscillator strength; for instance, these vibrations increase the oscillator strength from 0.5×10^{-4} and 0.3×10^{-4} to 5.2×10^{-4} and 2.8×10^{-4} for the $^1A_{1g} \rightarrow {}^1T_{1g}$ and $^1A_{1g} \rightarrow {}^1T_{2g}$ transitions, respectively, in $[Co(NH_3)_6]^{3+}$, when going from 0 to 293 K, as shown in Table 2. The significantly large increases by these vibrations arise from their very small wavenumbers of 42−128 and 47−107 cm^{-1} in $[Co(NH_3)_6]^{3+}$ and $[Rh(NH_3)_6]^{3+}$, respectively, as shown in Table 3.[29,30] Because of such small wavenumbers, the population of the vibrationally excited states considerably increases, when going from 0 to 293 K; for instance, these populations are 0.53−0.81 and 0.59−0.79 in $[Co(NH_3)_6]^{3+}$ and $[Rh(NH_3)_6]^{3+}$, respectively, at 293 K, which are much larger than their populations at the vibrational ground state, as shown in Table 3. Because the probability of the distorted geometry is much larger in the vibrationally excited state than in the ground state, the rotational vibration around the M−NH_3 bond axis contributes considerably to the oscillator strength at 293 K.

Besides the M−NH_3 rotational vibration, two kinds of H_3N−M−NH_3 antisymmetric bending vibrations of T_{1u} and T_{2u} moderately contribute to the increase in the oscillator strength, when going from 0 to 293 K, as shown in Table 2. The increase in the oscillator strength by these vibrations is somewhat smaller than that by the M−NH_3 rotational vibration. This is because the wavenumbers of these H_3N−M−NH_3 antisymmetric bending vibrations are much larger than that of the M−NH_3 rotational vibration, as shown in Table 3. As a result, the populations (0.24 in the T_{1u} mode and 0.36−0.38 in the T_{2u} mode) of the vibrationally excited states are much smaller in these antisymmetric bending vibrations than in the rotational vibration (0.53−0.81), and hence, the oscillator strength moderately increases by these bending vibrations when temperature goes up.

The wavenumber of the degenerate antisymmetric M−NH_3 stretching vibration is 400−402 cm^{-1} and 395−397 cm^{-1} in $[Co(NH_3)_6]^{3+}$ and $[Rh(NH_3)_6]^{3+}$, respectively,[31] which are considerably larger than those of the degenerate antisymmetric H_3N−M−NH_3 bending vibration and the M−NH_3 rotational vibration; see Table 3. The population of this vibrationally excited states is small (0.14) at 293 K in both complexes, as shown in Table 2. Thus, the degenerate antisymmetric M-NH_3 stretching vibration contributes much less to the increase in the oscillator strength than the degenerate antisymmetric H_3N-M-NH_3 bending and the M-NH_3 rotational vibrations, when going from 0 to 293 K; actually, this vibration increases the oscillator strength of the $^1A_{1g} \rightarrow {}^1T_{1g}$ transition by only 0.3×10^{-4} in $[Co(NH_3)_6]^{3+}$, as shown in Table 3. On the basis of these results, it is concluded that the degenerate antisymmetric M−NH_3 stretching mode contributes little to the oscillator strength of the d-d absorption at both 0 and 293 K, though the molecular distortion from the octahedral geometry is somewhat largely induced by this vibration mode.

The wavenumbers of the M−NH_3 wagging, N−H stretching, and N−H bending vibrations are significantly large, being more than 700 cm^{-1} in both of $[Co(NH_3)_6]^{3+}$ and $[Rh(NH_3)_6]^{3+}$, as shown in Table 3. Thus, the populations in their vibrationally excited states are nearly zero even at 293 K, and hence, these vibration modes contribute little to the increase in the oscillator strength, when going from 0 to 293 K.

MLCT Character in Symmetry-Forbidden d-d Transition. The t_{2g} and e_g Kohn−Sham orbitals of $[Co(NH_3)_6]^{3+}$ and $[Rh(NH_3)_6]^{3+}$ are presented in Figure 1. The e_g orbitals mainly consist of the d orbital of the metal center and moderately of the lone-pair orbitals of the NH_3 ligands, whereas the t_{2g} orbitals consist of the d orbital of the metal center only.

dx.doi.org/10.1021/ic2017402 | Inorg. Chem. 2012, 51, 2785−2792

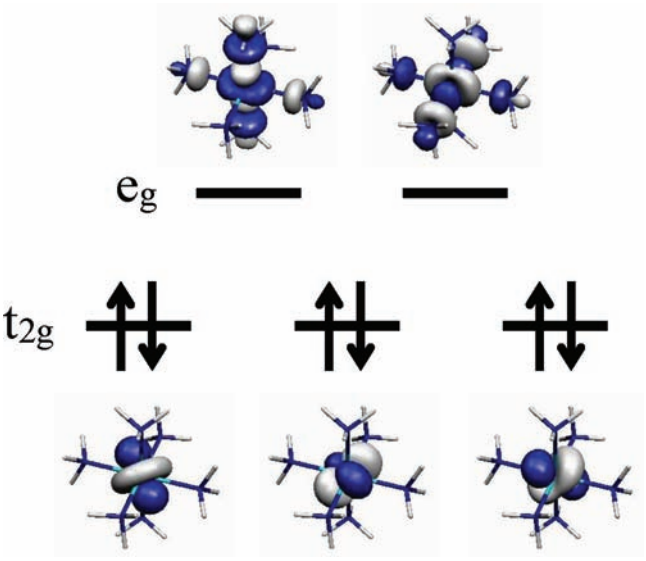

Figure 1. Kohn–Sham orbitals of $[Co(NH_3)_6]^{3+}$.

This means that the $^1A_{1g} \rightarrow {}^1T_{1g}$ and $^1A_{1g} \rightarrow {}^1T_{2g}$ transitions moderately contain metal-to-ligand charge transfer (MLCT) character from the d_{xy}, d_{yz}, and d_{xz} orbitals of the metal center to the lone-pair orbital of NH_3 ligand.

This MLCT character is larger in the $^1A_{1g} \rightarrow {}^1T_{1g}$ transition than in the $^1A_{1g} \rightarrow {}^1T_{2g}$ transition, as follows: In both of $[Co(NH_3)_6]^{3+}$ and the Rh analogue, the $^1A_{1g} \rightarrow {}^1T_{1g}$ transition decreases more the M atomic population and increases more the N atomic population than does the $^1A_{1g} \rightarrow {}^1T_{2g}$ transition, as shown in Table 4, where the Mulliken population analysis

Table 4. Mulliken Populations of Co, Rh, N, and H atoms[a] in the $^1A_{1g}$, $^1T_{1g}$, and $^1T_{2g}$ states of $[Co(NH_3)_6]^{3+}$ and $[Rh(NH_3)_6]^{3+}$

	Mulliken population			change of Mulliken population	
	$^1A_{1g}$	$^1T_{1g}$	$^1T_{2g}$	$^1A_{1g} \rightarrow {}^1T_{1g}$	$^1A_{1g} \rightarrow {}^1T_{2g}$
$[Co(NH_3)_6]^{3+}$					
Co	27.064	26.997	27.019	−0.067	−0.045
N	7.059	7.073	7.069	+0.014	+0.010
H	0.810	0.809	0.809	−0.001	−0.001
$[Rh(NH_3)_6]^{3+}$					
Rh	44.980	44.826	44.848	−0.154	−0.132
N	7.102	7.129	7.125	+0.027	+0.023
H	0.801	0.800	0.800	−0.001	−0.001

[a]Averaged values of 6 N atoms and 18 H atoms are presented here.

was employed; note that the change in the N atomic population directly relates to the extent of the CT to the lone pair orbital of NH_3.[32] Also, the $^1A_{1g} \rightarrow {}^1T_{1g}$ and $^1A_{1g} \rightarrow {}^1T_{2g}$ transitions decrease more the M atomic population and increase more the N atomic population in $[Rh(NH_3)_6]^{3+}$ than in $[Co(NH_3)_6]^{3+}$, as shown in Table 4. These results indicate that the MLCT character is larger in the $^1A_{1g} \rightarrow {}^1T_{1g}$ transition than in the $^1A_{1g} \rightarrow {}^1T_{2g}$ transition and larger in the d-d transitions of $[Rh(NH_3)_6]^{3+}$ than in those of $[Co(NH_3)_6]^{3+}$.

As the MLCT character increases, the oscillator strength increases in general. Actually, the extent of the MLCT character in the d-d transition is parallel to the oscillator strength of the d-d transition; remember that the oscillator strength of the $^1A_{1g} \rightarrow {}^1T_{1g}$ transition is larger than that of the $^1A_{1g} \rightarrow {}^1T_{2g}$ transition, and both of their oscillator strengths are larger in $[Rh(NH_3)_6]^{3+}$ than in $[Co(NH_3)_6]^{3+}$.

We wish to mention here the reason why the MLCT character is larger in the symmetry-forbidden d-d transition of $[Rh(NH_3)_6)]^{3+}$ than in that of $[Co(NH_3)_6)]^{3+}$. In general, the 4d transition metal forms stronger coordinate bond than the 3d transition metal because the 4d orbital expands more widely than the 3d orbital.[33] As a result, the 4d orbital of Rh overlaps with the lone pair orbital of NH_3 more than the 3d orbital of Co does, which leads to larger mixing of the NH_3 lone pair orbital into the d_{e_g} orbital in the Rh complex than in the Co analogue. Thus, the MLCT character is larger in the Rh complex than in the Co complex, which is responsible for the larger oscillator strengths of $[Rh(NH_3)_6)]^{3+}$ than those of $[Co(NH_3)_6)]^{3+}$.

CONCLUSIONS

We proposed here a new method to evaluate the oscillator strength of the symmetry-forbidden d-d transition of the transition metal complex bearing the inversion symmetry. In this method, the probability of distorted geometry is evaluated with the vibrational wave function, and the Boltzmann distribution law is employed to evaluate the population of the vibrationally excited state. The Herzberg–Teller approximation is not necessary here. We applied this method to the symmetry-forbidden d-d absorptions of such octahedral complexes as $[Co(NH_3)_6]^{3+}$ and $[Rh(NH_3)_6]^{3+}$. The present calculations reproduce the experimental results,[26,27] as follows: (i) The oscillator strengths of the $^1A_{1g} \rightarrow {}^1T_{1g}$ and $^1A_{1g} \rightarrow {}^1T_{2g}$ transitions agree well with the experimental results in $[Co(NH_3)_6]^{3+}$, while those of the Rh analogue are somewhat smaller than the experimental results. (ii) The oscillator strength of the $^1A_{1g} \rightarrow {}^1T_{1g}$ transition is considerably larger than that of the $^1A_{1g} \rightarrow {}^1T_{2g}$ transition in both of $[Co(NH_3)_6]^{3+}$ and $[Rh(NH_3)_6]^{3+}$. And, (iii) the oscillator strengths of these transitions are considerably larger in the Rh complex than in the Co complex.

In these complexes, the $H_3N–M–NH_3$ antisymmetric bending vibration (M = Co or Rh) contributes considerably to the oscillator strength of the d-d transition because the geometrical distortion is largely induced by this vibration. It is also noted that the $M–NH_3$ wagging vibration contributes considerably to the oscillator strength despite of moderate lowering of symmetry by this vibration and that the $M–NH_3$ antisymmetric stretching vibration contributes little to the oscillator strength despite of considerable lowering of symmetry by this vibration.

Interestingly, the oscillator strengths of the $^1A_{1g} \rightarrow {}^1T_{1g}$ and $^1A_{1g} \rightarrow {}^1T_{2g}$ transitions are evaluated to be considerably large even at 0 K in these complexes. The distorted geometry (or the geometry uncertainty) by the zero-point vibration is responsible for the oscillator strength of the symmetry-forbidden d-d transition at 0 K. When temperature goes up to 293 K, the oscillator strength increases. This increase in the oscillator strength is mainly induced by the $H_3N–M–NH_3$ antisymmetric degenerate bending vibrations of T_{1u} and T_{2u} symmetries, $M–NH_3$ wagging vibration, and $M–NH_3$ rotational vibration around the $M–NH_3$ bond axis. The MLCT character, which is involved in the symmetry-forbidden d-d transition, contributes to the oscillator strength of the d-d

dx.doi.org/10.1021/ic2017402 | Inorg. Chem. 2012, 51, 2785–2792

absorption. This character is larger in $[Rh(NH_3)_6]^{3+}$ than in $[Co(NH_3)_6]^{3+}$.

These results indicate that our method is useful in evaluating and understanding the oscillator strength of the symmetry-forbidden d-d transition. Our procedure is much simpler than the method with MD simulation and the Herzberg–Teller approximation. Though our procedure needs to calculate $f_{dist,i}(Q_i)$ value at many Q_i points, we can reduce this computation; see Supporting Information page S5. At the end of this paper, we wish to note again the presence of several weak-points in our method; see the section "Method and Computational Details".

■ ASSOCIATED CONTENT

Supporting Information

Full references of Gaussian 03 and Gaussian 09, the details of calculations, and the reduced computational procedure by using the relation, $f_{dist,i}(Q_i) = a_iQ_i^2$. This material is available free of charge via the Internet at http://pubs.acs.org.

■ AUTHOR INFORMATION

Corresponding Author

*E-mail: sakaki@moleng.kyoto-u.ac.jp.

Notes

The authors declare no competing financial interest.

■ ACKNOWLEDGMENTS

This work was financially supported by Grant-in-Aid on Specially Promoted Science and Engineering (No. 22000009), and Grand-Challenge Project from the Ministry of Education, Science, Sports, and Culture, and Research Fellowship of the Japan Society for the Promotion of Science for Young Scientists. Some of the theoretical calculations were performed with SGI workstations of the Institute for Molecular Science (Okazaki, Japan), and some of them were carried out with PC cluster computers in our laboratory.

■ REFERENCES

(1) Grimme, S. *Rev. Comput. Chem.* **2004**, *20*, 153.

(2) Ehara, M.; Hasegawa, J.; Nakatsuji, H. *SAC-CI method applied to molecular spectroscopy*. In *Theory and Applications of Computatinal Chemistry: The First Forty Years*; Dyksrtra, C. E., Frenking, F., Kim, K. S., Scuseria, G. E., Eds.; Elsevier: Oxford, U.K., 2005; p 1099.

(3) Figgs, B. N.; Hitchman, M. A. *Ligand-Field Theory and its Applications*; Wiley: New York, 2000.

(4) Sugano, S.; Tanabe, Y.; Kamimura, H. *Multiplets of Transition-metal Ions in Crystals*; Academic Press Inc.: New York, *1970*.

(5) (a) Iuchi, S.; Morita, A.; Kato, S. *J. Chem. Phys.* **2004**, *121*, 8446. (b) Iuchi, S.; Sakaki, S. *Chem. Phys. Lett.* **2010**, *485*, 114.

(6) Bridgeman, A. J. *Inorg. Chem.* **2008**, *47*, 4817.

(7) Hertzberg, G.; Teller, E. *Z. Phys. Chem., Abt. B* **1933**, *21*, 410.

(8) According to the Herzberg–Teller (HT) approximation, the transition dipole M is represented, as follows; $M = M(0) + \sum_i (\partial M/\partial Q_i)_0 Q_i$, where the Q_i is the normal coordinate of fundamental vibration mode i and the subscript "0" represents the equilibrium geometry. The transition dipole M is calculated, as follows: $M = \sum_i (\partial M/\partial Q_i)_0 \langle \chi_{0,i}(Q_i)|Q_i|\chi_{e,i}(Q_i)\rangle$, where $\chi_{0,i}$ and $\chi_{e,i}$ represent fundamental vibrational functions at the electronic ground and the excited states, respectivey.

(9) $[Co(NH_3)_6]^{3+}$ and $[Rh(NH_3)_6]^{3+}$ are not O_h symmetrical strictly speaking but C_i symmetrical in the equilibrium geometry. However, the C_i symmetry arises from the presence of the H atoms of NH_3 ligands, and the main flame is O_h symmetrical. Hence, the terms of $^1A_{1g}$, $^1T_{1g}$, and $^1T_{2g}$ were used here; in other words, the ground state was named as $^1A_{1g}$ and the excited states were named as $^1T_{1g}$ and $^1T_{2g}$ in both of $[Co(NH_3)_6]^{3+}$ and $[Rh(NH_3)_6]^{3+}$.

(10) Dolg, M.; Wedig, U.; Stoll, H. *J. Chem. Phys.* **1987**, *86*, 866.

(11) Andrae, D.; Haeussermann, U.; Dolg, M.; Stoll, H.; Preuss, H. *Theor. Chim. Acta* **1990**, *77*, 123.

(12) Martin, J. M. L.; Sundermann, A. *J. Chem. Phys.* **2001**, *114*, 3408.

(13) Dunning, T. H. Jr. *J. Chem. Phys.* **1989**, *90*, 1007.

(14) (a) Becke, A. D. *Phys. Rev. A* **1988**, *38*, 3098. (b) Becke, A. D. *J. Chem. Phys.* **1993**, *98*, 5648.

(15) Perdew, J. P.; Wang, Y. *Phys. Rev. B* **1992**, *45*, 13244.

(16) Casida, M. E. *Recent Advances in Density Functional Methods, Part I*; Chong, D. P., Ed.; World Scientific: Singapore, 1995.

(17) Gross, E. U. K.; Dobson, J. F.; Petersilka, M. *Density Functional Theory II*; Nalewajski, R. F., Ed.; Springer: Heideberg, Germany, 1996.

(18) (a) Pople, J. A.et al. *Gaussian 03*, Revision D.02; Gaussian, Inc.: Wallingford, CT, 2004. (b) Frisch, M. J. et al. *Gaussian 09*, revision A.02; Gaussian, Inc.: Wallingford, CT, 2009.

(19) Scott, A. P.; Radom, L. *J. Phys. Chem.* **1996**, *100*, 16502.

(20) (a) Flükiger, P.; Lüthi, H. P.; Portmann, S.; Weber, J. *MOLEKEL*, version 4.3; Scientific Computing: Manno, Switzerland, 2000–2002. (b) Portmann, S.; Lüthi, H. P. *CHIMIA* **2000**, *54*, 766.

(21) We must consider the potential energy surface and vibrational wave function in the excited state, strictly speaking. For instance, a probability of distorted geometry in the excited state, which is given by the $g(Q)$-type function of eq 1, must be considered, because the d-d transition may become allowed due to odd vibrations not only in the ground state but also in the excited state. However, it is not easy to present correctly the potential energy surface of the excited states of $[Co(NH_3)_6]^{3+}$ and the Rh analogue, because we must use the Multi-State-CASPT2 method to evaluate such potential energy surface including the Jahn–Teller distortion; note that the use of Multi-State-CASPT2 calculation of the excited state is not easy. Because of these weak-points discussed here and in the text, we need to further develop the method to incorporate these factors in the future.

(22) (a) Bersuker, I. B.; Polinger, V. Z. *Vibronic Interactions in Molecules and Crystals*; Springer: New York, 1989. (b) Bersuker, I. B. *The Jahn-Teller Effect*; Cambridge University Press: Cambridge, England, 2006. (c) Solomon, E. I.; Hanson, M. A. Bioinorganic Spectroscopy. In *Inorganic Electronic Structure and Spectroscopy, Vol. II: Applications and Case Studies*; Solomon, E. I., Lever, A. B. P., Eds.; Wiley: NJ, 2006.

(23) Because the oscillator strengths $f_{dist,i}(\pm Q_{i,avg,0})$ and $f_{dist,i}(\pm Q_{i,avg,1})$ are much small (less than 10^{-4}), these values cannnot be presented by the TD-DFT calculations under the default conditions of Gaussian 03 and 09 programs; for example, the calculated oscillator strength less than 0.00005 is displayed as "0.0000" in the output file of the default Gaussian 03 and 09. To present such small oscillator strengths, we modified the setting of Gaussian 03 and 09.

(24) Meek, D. W.; Ibers, J. A. *Inorg. Chem.* **1970**, *9*, 465.

(25) Kimura, T.; Sakurai, T. *J. Solid. State. Chem.* **1980**, *34*, 369.

(26) (a) Kofod, P. *Inorg. Chem.* **1995**, *34*, 2768. (b) The oscillator strength was evaluated from the spectrum reported here.

(27) (a) Peterson, J. D.; Ford, P. C. *J. Phys. Chem.* **1974**, *78*, 1144. (b) The oscillator strength was evaluated from the spectrum reported here.

(28) (a) One of the plausible origins of the smaller calculated oscillator strength than the experimental value in the Rh complex is the neglect of the spin-orbit interaction, because the spin-forbidden symmetry-allowed state can mix into the spin-allowed symmetry-forbidden d-d excitation state through spin-orbit interaction. The other plausible origin is the weak point of the TD-DFT method.[28b] In general the TD-DFT method tends to present a small transition dipole.[28c] Moreover, in the Rh complex, the d-d transition contains larger CT character than in the Co complex because the orbital overlap between the d orbital and NH_3 lone pair orbital is larger than in the Co complex. The TD-DFT calculation tends to present a poor result for a CT transition[28d] without the range-corrected exchange functional.[28e] (b) Recent review: Cramer, C. J.; Truhlar, D. G. *Phys. Chem. Chem. Phys.* **2009**, *11*, 10757. (c) Appel, F.; Gross, E. K. U.;

Burke, K. *Phys. Rev. Lett.* **2003**, *90*, 043005. (d) Dreuw, A.; Weisman, J. L.; Head-Gordon, M. *J. Chem.. Phys.* **2003**, *119*, 2943. (e) Tawada, Y.; Tsuneda, T.; Yanagisawa, S.; Yanai, T.; Hirao, K. *J. Chem. Phys.* **2004**, *120*, 8425.

(29) $[Co(NH_3)_6]^{3+}$ and $[Rh(NH_3)_6]^{3+}$ have three fundamental vibration modes of the T_{1u} H_3N-M-NH_3 antisymmetric degenerate bending vibration. Their oscillator strengths presented in Table 2 are the sum of the oscillator strengths provided by three fundamental bending vibrations in the T_{1u} mode; for example, the oscillator strength of the $^1A_{1g} \rightarrow {}^1T_{1g}$ transition of $[Co(NH_3)_6]^{3+}$ by this vibration is 1.2×10^{-4} which is the sum of three oscillator strengths (0.4×10^{-4}) induced by three T_{1u} vibrations.

(30) $[Co(NH_3)_6]^{3+}$ and $[Rh(NH_3)_6]^{3+}$ have three fundamental rotational vibrations around the M-NH_3 axis with ungerade symmetry. Wavenumbers of these fundamental vibrations are 42, 44, and 128 cm^{-1} in $[Co(NH_3)_6]^{3+}$ and 47, 48, and 107 cm^{-1} in $[Rh(NH_3)_6]^{3+}$. We reported here their wavenumbers as 42−128 cm^{-1} and 47−107 cm^{-1}, respectively, for brevity. The wavenumbers of the other molecular vibrations are also provided in the similar way.

(31) Because $[Co(NH_3)_6]^{3+}$ and $[Rh(NH_3)_6]^{3+}$ are not completely O_h symmetrical strictly speaking, the H_3N-M-NH_3 antisymmetric bending (T_{1u} and T_{2u}) and M-NH_3 antisymmetric streching (T_{1u}) vibrations are not completely degenerate. However, these fundamental vibrations exhibit similar frequency values to each other; for example, the wavenumbers of the T_{2u} bending mode are 199, 209, and 209 cm^{-1} in $[Co(NH_3)_6]^{3+}$ and 189, 196, and 196 cm^{-1} in $[Rh(NH_3)_6]^{3+}$, indicating that the discussion can be presented based on the O_h symmetry; see also ref 9.

(32) Because the lone pair orbital of NH_3 participates in the bonding interaction with the d_{e_g} orbital of the metal center, the Mulliken population of the H atom hardly changes in both transitions. Thus, the change in N atomic population corresponds to the CT from the NH_3 lone pair to the metal center.

(33) Frenking, G.; Frohlich, N. *Chem. Rev.* **2000**, *100*, 717.